Efflux-dependent auxin gradients establish the apical–basal axis of *Arabidopsis*

Jiří Friml[1]*, **Anne Vieten**[1]*, **Michael Sauer**[1]*, **Dolf Weijers**[1,2], **Heinz Schwarz**[3], **Thorsten Hamann**[1]†, **Remko Offringa**[2] & **Gerd Jürgens**[1]

[1]*Zentrum für Molekularbiologie der Pflanzen, Universität Tübingen, Auf der Morgenstelle 3, 72076 Tübingen, Germany*
[2]*Institute of Biology, Clusius Laboratory, Leiden University, Wassenaarseweg 64, 2333 AL, Leiden, The Netherlands*
[3]*Max Planck Institute for Developmental Biology, Spemannstrasse 35, D-72076 Tübingen, Germany*

* These authors contributed equally to this work
† Present address: Department of Plant Biology, Carnegie Institution of Washington, 260 Panama street, 94305 Stanford, USA

....

Axis formation occurs in plants, as in animals, during early embryogenesis. However, the underlying mechanism is not known. Here we show that the first manifestation of the apical–basal axis in plants, the asymmetric division of the zygote, produces a basal cell that transports and an apical cell that responds to the signalling molecule auxin. This apical–basal auxin activity gradient triggers the specification of apical embryo structures and is actively maintained by a novel component of auxin efflux, PIN7, which is located apically in the basal cell. Later, the developmentally regulated reversal of PIN7 and onset of PIN1 polar localization reorganize the auxin gradient for specification of the basal root pole. An analysis of *pin* quadruple mutants identifies PIN-dependent transport as an essential part of the mechanism for embryo axis formation. Our results indicate how the establishment of cell polarity, polar auxin efflux and local auxin response result in apical–basal axis formation of the embryo, and thus determine the axiality of the adult plant.

The development of higher eukaryotes includes the generation of a species-specific body plan. As a first step, a multicellular organization is established from a single-celled zygote during embryogenesis, with cells adopting specific fates according to their relative positions. In *Drosophila*, maternal organizers initiate a cascade of spatially restricted transcription factors that partitions the anterior–posterior axis of the embryo[1]. In *Caenorhabditis elegans*, sperm entry triggers anterior–posterior axis specification, initiating a series of asymmetric cell divisions that establish founder cells with different fate potential[2]. In plants, the mature embryo displays a main axis of polarity, with the shoot meristem flanked by the cotyledons (embryonic leaves) at the top end and separated by hypocotyl (embryonic stem) and root from the root meristem at the opposite pole. The origin of this apical–basal pattern, which is remarkably uniform across flowering plant species, has been traced back to early embryogenesis in *Arabidopsis*[3]. The zygotic division generates a smaller apical and a larger basal cell. The apical cell divides vertically and eventually gives rise to all apical embryo structures. The basal cell continues to divide horizontally and produces the suspensor, which connects the embryo with the maternal tissue[3]. The uppermost suspensor cell is subsequently recruited by the embryo and specified to become the hypophysis—the founder of the root meristem. At the triangular stage, the apical pole of the embryo is organized with the initiation of two symmetrically positioned cotyledons.

Several indirect lines of evidence implicated the plant hormone auxin (indole-3-acetic acid, IAA) in embryo development. Embryo patterning mutants, such as *monopteros* (*mp*), *bodenlos* (*bdl*) or *gnom* (*gn*)[4,5], lack basal structures and display variably fused cotyledons. Molecular analysis of these mutants has revealed that *MP* and *BDL* encode the transcriptional activator auxin response factor 5 (ARF5) and the corresponding transcriptional repressor IAA12, respectively, both of which are involved in auxin response[6,7], and that *GN* encodes a regulator of vesicle trafficking that mediates the subcellular targeting of auxin-transport components[8,9]. For later development, chemical manipulation of auxin distribution has

suggested a link between patterning and auxin transport[10–13]. Moreover, in wheat and carrot later-stage embryos, auxin has been detected using a microscale technique[14,15].

Auxin is actively distributed within the plant by efflux-dependent cell-to-cell movement[16]. The direction of auxin flow was proposed to be determined by the asymmetric cellular localization of efflux carriers[17,18], probably represented by plant-specific PIN proteins[19]. However, reported *pin* mutants[13,20] as well as other auxin transport or response mutants display only mild and infrequent early embryonic defects. Moreover, the presence of auxin or its response has not been demonstrated in early embryogenesis. Thus, the function of auxin in apical–basal pattern formation during embryogenesis of higher plants is debatable, and the process of early pattern formation itself is mechanistically only poorly understood.

Here we show dynamic gradients of auxin accumulation and response during *Arabidopsis* early embryogenesis, which are mediated by cellular efflux and required for apical–basal axis formation. A novel auxin efflux regulator, PIN7, and other functionally redundant PIN proteins are important determinants of both auxin gradients and apical–basal axis establishment. Our results suggest a model of how spatially separated auxin transport and response from the zygotic division onwards, together with the establishment of cell polarity, mediate patterning along the initial apical–basal auxin gradient.

Apical–basal auxin gradients in embryogenesis

The activity of the synthetic auxin-responsive promoter *DR5* has been used to visualize the spatial pattern of auxin response, and hence indirectly the distribution of auxin[12,13,21,22]. We constructed a fluorescent variant, *DR5rev::GFP*, which enabled us to monitor auxin response and its dynamics from the earliest stages of embryogenesis onwards. Immediately after the division of the zygote, *DR5* activity was pronounced in the smaller, apical cell (Fig. 1a). Signal intensity rapidly increased in the developing proembryo, whereas only very weak signal was detected in the suspensor (Fig. 1b, c). This apical–basal auxin response gradient was reversed at around the

147

32-cell stage: the maximum of *DR5* activity shifted basally into the uppermost suspensor cells, including the hypophysis (Fig. 1d, e). At later stages of embryogenesis, additional *DR5* signals appeared in the tips of the developing cotyledons and in the provascular strands (Fig. 1f). When the quiescent centre of the root meristem was established, the *DR5* maximum shifted further basally into the adjacent columella precursors (Fig. 1f, inset). *DR5* activity persisted in these cells, showing the pattern previously reported for post-embryonic development[12,13,23].

Several controls were performed to examine whether *DR5rev::GFP* acted as a reliable reporter not only for auxin response but also for cellular auxin levels. First, exogenously supplied auxin induced *DR5* activity in all embryo cells (Fig. 2d), suggesting that the spatially restricted signals in untreated embryos reflected differences in auxin levels between cells. Second, another *DR5* variant and another reporter—the diphtheria toxin (DTA), a highly sensitive, non-fluorescent reporter that causes cell lethality[24]—were used. DTA expression by the *DR5* promoter was made conditional through the GAL4/*UAS* transactivation system[25]. In control experiments, β-glucuronidase (GUS) activity in DR5≫GUS embryos was undetectable before the late globular stage (not shown), whereas experiments with other activator lines revealed *UAS* transcription to be activated with variable strength and timing in sibling embryos[26,27]. This variation in both onset and strength of GAL4/*UAS* transactivation enabled us to assess DTA effects at different

stages of embryogenesis. DTA expression before the globular stage caused mainly symptoms of ablation in apical cells, as visualized by the enhanced nuclear fluorescence of Schiff staining (Fig. 1g). By contrast, later DTA expression led exclusively to defects in the basal region (Fig. 1h, compare with Fig. 4a). Thus, the *DR5≫DTA* reporter displayed the same spatiotemporal activity pattern as the *DR5rev::GFP* reporter. Finally, we monitored the accumulation of auxin itself by immunolocalization with an anti-IAA antibody[28]. Increased IAA levels were detected apically in the pre-globular embryo (Fig. 1i), whereas the basal part of the embryo stained strongly from the globular stage onwards (Fig. 1j). Later, the IAA maximum moved from the quiescent centre of the root meristem into the columella precursors (Fig. 1j, inset), as observed for DR5 (see Fig. 1f, inset). Thus, the dynamic IAA accumulation pattern mirrored the *DR5* activity pattern, confirming the apical–basal reversal of auxin distribution and response during early embryogenesis.

Cellular efflux links auxin gradients and patterning

Experimental manipulation of auxin homeostasis in the tiny *Arabidopsis* embryo has not been possible so far. We established *in vitro* culture of embryos within excised ovules. Cultured embryos developed normally and displayed the stage-specific patterns of *DR5* activity (Fig. 2f). To examine whether auxin transport has a role in *DR5* activity distribution, embryos were cultured in the presence of synthetic auxins, the efflux substrate 1-naphthaleneacetic acid (NAA) or the influx substrate 2,4-dichlorophenoxyacetic acid (2,4-D)[29]. NAA increased *DR5* activity without changing its pattern (Fig. 2a, c). By contrast, 2,4-D interfered with the *DR5* pattern, resulting in a strong signal in the entire embryo (Fig. 2d). Inhibiting auxin efflux either by the phytotropin NPA or the vesicle-trafficking inhibitor brefeldin A (BFA) perturbed the *DR5* pattern. At early
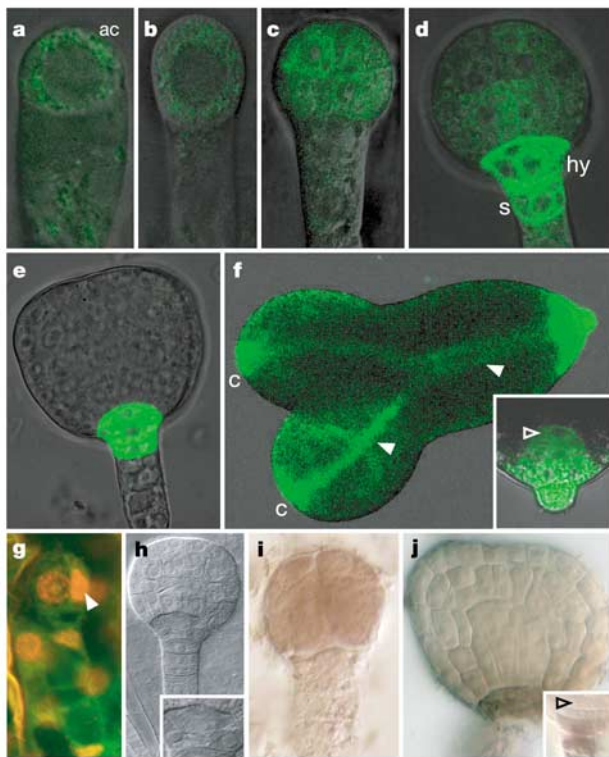
Figure 1 Auxin and auxin response in embryogenesis. **a**–**f**, *DR5rev::GFP* auxin response. Maximum in the apical cell (ac) lineage after zygotic division (**a**), and at the one-cell (**b**) and the eight-cell (**c**) stage. Shift to the hypophysis (hy) and upper suspensor (s) cells in young globular (**d**) and triangular (**e**) embryos. Additional signals in cotyledon (c) tips and provasculature (arrowheads) at the torpedo stage (**f**); inset, maximum below the quiescent centre (open arrowhead). **g**, **h**, *DR5≫DTA* expression. Apical defects in young embryos (**g**); arrowhead, dying proembryo cell. Basal defects in globular embryo (**h**). **i**, **j**, IAA accumulation in a 16-cell-stage proembryo (**i**), at the basal pole of a triangular embryo (**j**), and below the quiescent centre (open arrowhead) at the torpedo stage (inset). GFP fluorescence in green (**a**–**f**). Schiff staining in red (**g**). IAA signals in brown (**i**, **j**).
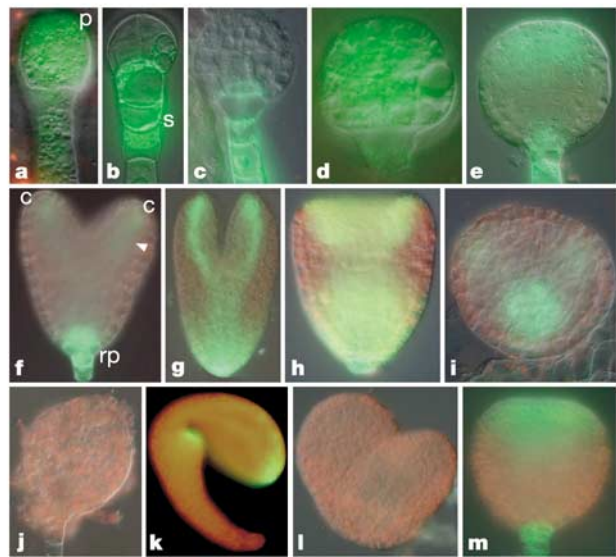
Figure 2 *DR5* auxin response in *in vitro* cultured ovules and mutants. **a**, **b**, Pre-globular embryos treated with: NAA, enhanced signal in proembryo (p) (**a**); NPA, ectopic suspensor (s) signal (**b**). **c**–**e**, Globular embryos treated with: NAA, enhanced basal signal (**c**); 2,4-D, ubiquitous signal (**d**); BFA, ectopic apical signal (**e**). **f**, Untreated heart-stage embryo. DR5 signals at the root pole (rp), cotyledon (c) tips and weaker in provascular tissue (arrowhead). **g**–**i**, Long-term treatment with: NAA, enhanced signal but no change in spatial pattern (**g**); 2,4-D, abnormal *DR5* activity, cotyledon and root pole specification compromised (**h**); BFA, in extreme cases, no apical–basal axis establishment (**i**). **j**–**m**, No basal signal in *mp* (**j**, **k**) or *bdl* (**l**) embryos, occasional signal in developing cotyledon tips (**k**), ectopic apical signal in *gn* embryos (**m**). Times of culture: 16 h (**a**–**e**), 3 days (**f**–**i**). GFP fluorescence in green. Autofluorescence in red.

stages, GFP (green fluorescent protein) fluorescence was detected in the suspensor (Fig. 2b, compare with Fig. 2a) rather than in the proembryo, whereas after reversal of the gradient, an ectopic *DR5* maximum appeared in the embryo apex (Fig. 2e, compare with Fig. 1d, e). These data strongly suggest that the auxin distribution in embryos, as reflected by *DR5* activity, is mediated by auxin efflux.

Long-term interference with auxin homeostasis enabled us to assess the relationship between auxin gradients and embryo patterning. NAA had no adverse effects (Fig. 2g). By contrast, the auxin analogue 2,4-D (Fig. 2h) as well as auxin-efflux inhibitors NPA and BFA (Fig. 2i) caused abnormalities in auxin distribution, which were always accompanied by embryo defects, ranging from cup-shaped embryos with misspecified apical structures and a non-functional root pole, to ball-shaped embryos without any discernible apical–basal axis. These defects resembled the phenotypes of *gn* and shared some features, such as lack of a functional root, with *mp* and *bdl*. In *mp* and *bdl* mutants, neither the early apical *DR5* activity nor the later basal *DR5* maximum was detectable (Fig. 2j, l). Only occasionally did older embryos show GFP expression at the tips of cotyledons (Fig. 2k), suggesting an involvement of other components of auxin response late in embryogenesis. *gn* mutants displayed a severely altered *DR5* activity pattern at the globular stage. Both the ectopic *DR5* maximum in the apical part of the embryo and the abnormally positioned peak in the suspensor mirrored the *DR5* activity pattern upon auxin-efflux inhibition (Fig. 2m, compare to Fig. 2e). Thus, both drug treatments and the analysis of embryo mutants correlated apical–basal patterning and cotyledon specification with spatial patterns of auxin distribution and response.
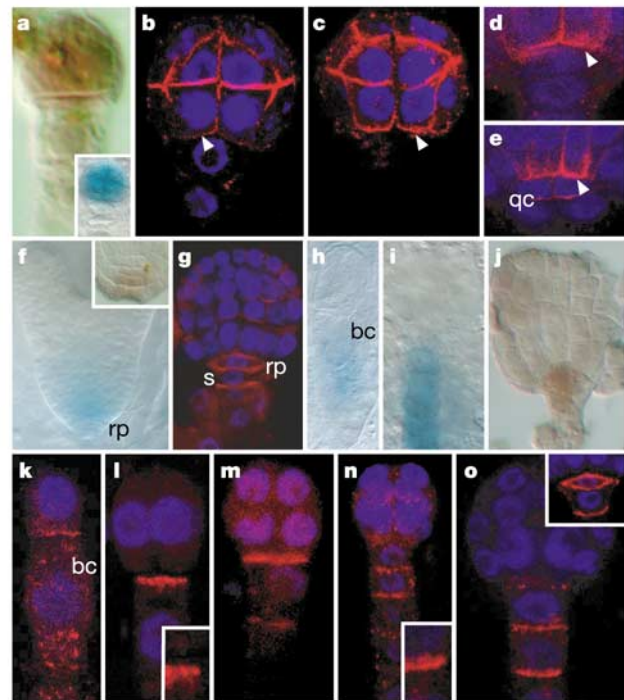
PIN expression in embryogenesis

To identify the molecular components of auxin efflux that mediate the dynamic auxin gradients in embryogenesis, we analysed the expression and function of PIN regulators of auxin efflux. Four out of eight *Arabidopsis PIN* genes, *PIN1–PIN4*, have been described[16]. We isolated full-length complementary DNAs for the novel members *PIN5–PIN8*. By sequence analysis, PIN5 and PIN8 are divergent family members that lack important domains and may have other functions. For the other six, we analysed the expression during embryogenesis using *PIN::GUS* transgenic plants, *in situ* hybridization and/or immunolocalization experiments. On the basis of *promoter::GUS* studies, neither *PIN2* nor *PIN6* expression was detectable in embryos (not shown). *PIN1::GUS* activity as well as *PIN1* messenger RNA was detected in the apical cell lineage (Fig. 3a). The earliest activity of *PIN3::GUS* was detected at the basal pole of the heart-stage embryo, confirmed by *PIN3* mRNA localization in the precursors of the columella (Fig. 3f). PIN4 protein localized to the descendants of the hypophysis and to provascular initials of the root meristem (Fig. 3g), as previously reported[13]. The novel gene *PIN7* displayed an expression pattern complementary to that of *PIN1*. A *Ds-GUS* enhancer-trap insertion[30] marked the basal cell lineage from the zygotic division onwards (Fig. 3h), which was confirmed for later stages by the expression pattern of a PIN7:GUS translational fusion (Fig. 3i) and by *PIN7* mRNA *in situ* hybridization (Fig. 3j). Thus, at least four *PIN* genes are expressed during embryogenesis, providing a system for regulated auxin distribution.

PIN polarity correlates with auxin distribution

Asymmetric subcellular localization of PIN proteins has been correlated with the direction of auxin flow in postembryonic development[16]. We therefore examined whether PIN1 and PIN7 localization correlated with the apical–basal auxin gradients in early embryogenesis. From the one-cell to the 16-cell stage, PIN1 marked all newly formed cell boundaries within the proembryo, without any detectable polarity (Fig. 3b). At the 32-cell stage, PIN1 became

polarly localized in the provascular cells facing the basal embryo pole—the hypophysis (Fig. 3c). This event coincided with the basal shift of the auxin response maximum to the hypophysis (see Fig. 1d). Within the forming root meristem, PIN1 also shifted to the basal side of the quiescent centre cells (Fig. 3d, e), which again coincided with the shift of the auxin maximum to the basally adjacent columella precursors (see Fig. 1f, j, insets).

To immunolocalize PIN7 protein in the embryo, we raised anti-PIN7 antiserum. PIN7 was detected in the basal cell immediately after the zygotic division, both in endomembranes and at the boundary facing the smaller apical cell (Fig. 3k), which was complementary to the auxin response maximum in the apical cell (see Fig. 1a). Until the 32-cell stage, PIN7 continued to reside at the apical side of suspensor cells facing the developing proembryo (Fig. 3l, m). Thus, PIN7 localization reflects early polarization of basal cells, representing the earliest polarity marker known. At around the 32-cell stage, the asymmetric localization of PIN7 suddenly reversed, shifting to the basal side of suspensor cells (Fig. 3n) for the rest of embryogenesis (Fig. 3o). After formation of the lens-shaped cell, PIN7 localized to all its boundaries (Fig. 3o, inset). Most interestingly, onset of the basal accumulation of PIN1 in the proembryo cells and reversal of PIN7 polarity correlated with the apical-to-basal reversal of the auxin gradient.


Figure 3 PIN expression and protein localization in embryogenesis. **a**, *PIN1* mRNA in a two-cell-stage proembryo, and *PIN1::GUS* (inset) in an eight-cell-stage proembryo. **b–e**, PIN1 protein at the inner cell boundaries of a 16-cell-stage proembryo (**b**), basally in provascular initials (arrowheads) of 16/32-cell-stage (**c**) and globular (**d**) embryos, and additional signals in the quiescent centre (qc) at the heart stage (**e**). **f**, *PIN3::GUS* and *PIN3* mRNA (inset) at the root pole (rp) of a heart-stage embryo. **g**, PIN4 protein at the basal end of provascular initials, at the root pole and in the uppermost suspensor (s) cell of a globular embryo. **h–j**, *PIN7* expression in the basal cell (bc) lineage. *Ds-GUS* enhancer-trap line, one-cell-stage (**h**); PIN7:GUS, globular embryo (**i**); *PIN7* mRNA, triangular embryo (**j**). **k–o**, PIN7 protein in the basal cell (bc) of a one-cell embryo (**k**); apically in the basal cell of two-cell (**l**) and eight-cell (**m**) embryos; basally in suspensor cells of 16/32-cell (**n**) and globular (**o**) embryos, and around a lens-shaped cell (inset). mRNA signals in brown (**a**, inset **f**, **j**). Protein signals in red and DAPI nuclear counterstain in blue (**b–e**, **g**, **k–o**). GUS staining in blue (**a**, inset **f**, **h**, **i**).

articles

Apical–basal pattern defects in *pin* mutants

To investigate the biological function of *PIN7*, we isolated three mutant alleles with insertions within the coding region (*pin7-1*, *-2* and *-3*) and generated *PIN7* RNAi (RNA interference) transgenic plants. RNA and protein analyses confirmed that the mutant alleles were null (not shown). The temporal and spatial correlation of PIN7 polar localization with auxin gradients suggests an involvement of PIN7 in this distribution. Therefore, we examined *DR5rev::GFP* expression in *pin7* early embryogenesis. Whereas wild-type embryos accumulated GFP in the apical cell lineage (see Fig. 1a–c), more than half of the *pin7* embryos failed to establish the apical–basal auxin gradient (Fig. 4l; Supplementary Table), similar to embryos treated with auxin-efflux inhibitors (see Fig. 2b). This demonstrates a role for PIN7-dependent efflux in mediating the initial auxin gradient in early embryogenesis.

By comparison with their respective wild-type parental lines (Fig. 4a), the stereotypical pattern of early embryogenesis was affected in all *pin7* mutant lines as well as in *PIN7* RNAi embryos

(Supplementary Table). Specification of the apical daughter cell of the zygote was compromised, as demonstrated by horizontal instead of vertical division (Fig. 4d, compare with Fig. 4a) as well as by uniform expression of the basal cell marker *PIN7-Ds-GUS* (Fig. 4i, compare with Fig. 3h). Occasionally, *pin7* embryos failed to establish the proembryo completely, resembling filamentous structures at later stages (Fig. 4b, c). In most cases, the defects were confined to the lower region of the proembryo. This was demonstrated morphologically (Fig. 4d) and also by PIN1 and *PIN1::GUS* apical markers, which frequently failed to be expressed in the lower region (Fig. 4j, k, compare with Fig. 3a, b). In some cases, two proembryos developed on top of each other (Fig. 4d). The lower proembryo usually developed more slowly and often retained morphological characteristics of a suspensor, as if the boundary between apical and basal embryo structures was not clearly defined. These defects strongly resembled other auxin-related mutants, such as *mp*, *bdl* and *gn*[31] (Fig. 4m–o). Nonetheless, a detailed comparison of embryo phenotypes in these mutants revealed that preglobular defects in
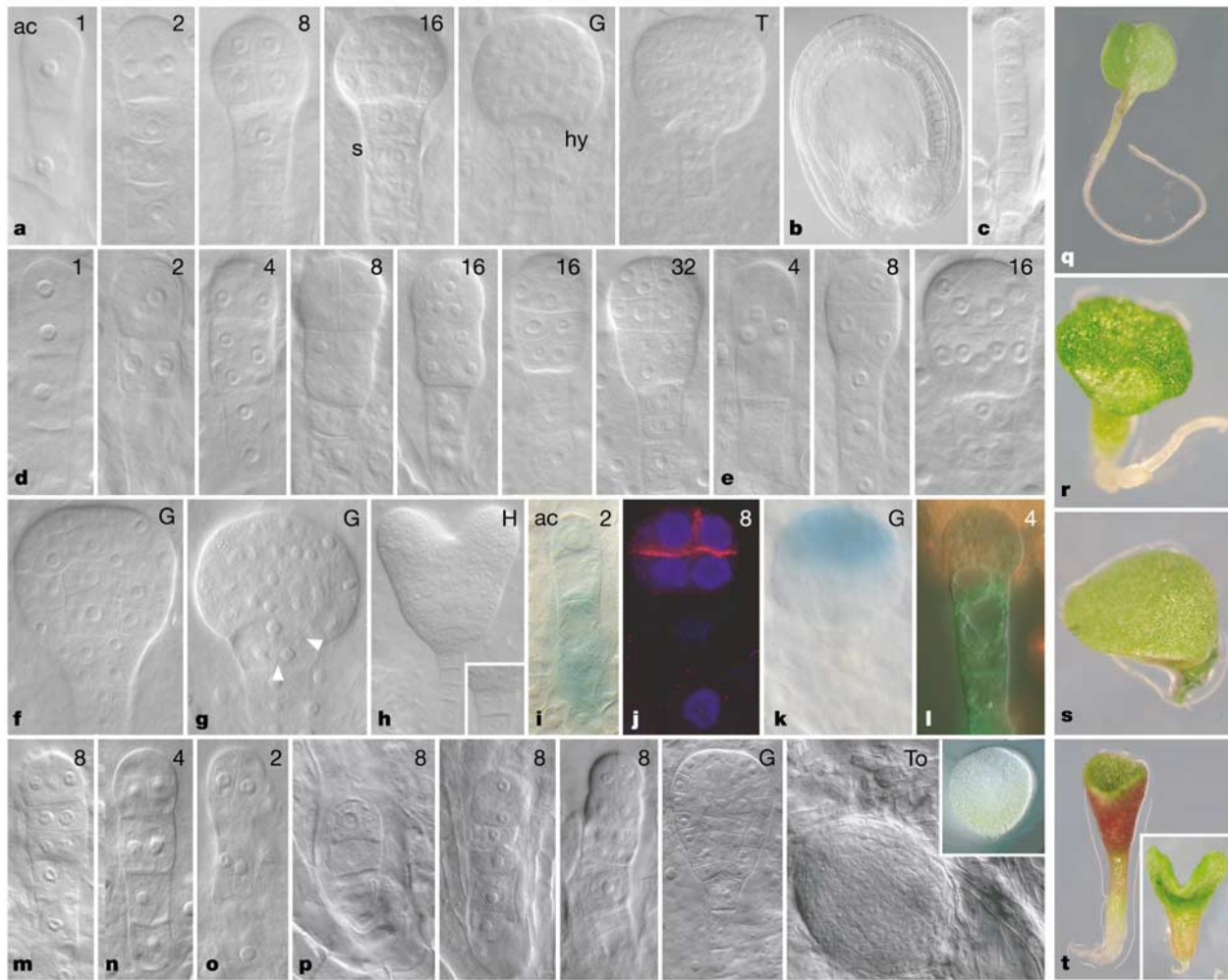
Figure 4 Abnormal embryogenesis in auxin transport and response mutants. **a**, Wild-type development. **b–e**, *pin7* mutants. Filamentous embryos with no apical cell established (**b**, **c**). Apical–basal boundary ill-defined (**d**), weaker defects in apical parts (**e**). **f–h**, Recovery of *pin7* proembryo after the globular stage (**f**), mild basal defects. Enlarged root pole with premature hypophysis division (**g**, arrowheads), abnormal cell divisions in the suspensor (**h**, inset). **i–l**, Abnormal marker expression in *pin7*. *PIN7-Ds-GUS* misexpressed in the apical cell (ac) (**i**), reduced apical domains of PIN1 (**j**) and *PIN1::GUS* (**k**), *DR5rev::GFP* ectopic expression in suspensor (**l**). **m–o**, Early defects in *mp* (**m**), *bdl* (**n**) and *gn* (**o**) mutants. **p**, Compromised apical–basal axis in *pin1 pin3 pin4 pin7*

embryos; inset, *gn* ball-shaped embryo. **q–t**, *pin* multiple mutant seedling phenotypes. Cotyledon defects in *pin4 pin7* (**q**), apical defects and short root in *pin1 pin3 pin4* (**r**), *pin1 pin3 pin4 pin7* stronger (**s**) and weaker (**t**) phenotypes; inset, *gn* seedling. GUS staining in blue (**i**, **k**). Protein signal in red and DAPI nuclear counterstain in blue (**j**). GFP fluorescence in green (**l**). For embryo stages, numbers indicate the developmental stage according to actual number of proembryo cells of the corresponding wild-type stage: G, globular; T, triangular; H, heart; To, torpedo. Apical cell (ac), suspensor (s) and hypophysis (hy) are marked.

pin7 embryos were stronger and more penetrant (Supplementary Table). At the globular stage, *mp*, *bdl* and *gn* showed fully penetrant defects in the specification of the hypophysis, probably being the cause of the postembryonic rootless phenotype in these mutants. By contrast, *pin7* started to recover at the globular stage (Fig. 4f), coinciding with the onset of PIN1 basal localization, PIN4 expression and reversal of the auxin gradient. From then on, developmental aberrations were confined to the basal part of the embryo (Supplementary Table). The region of the hypophysis was enlarged and premature cell divisions occurred (Fig. 4g), accompanied by aberrant cell divisions in the suspensor (Fig. 4h, inset).

Mild defects at the basal embryo pole were also observed in the *pin1* mutant. Whereas the hypophysis was established and divided in about half of the globular and in all triangular wild-type embryos, this was the case for only about one-quarter and two-thirds of the respective embryos from *pin1/PIN1* plants (Supplementary Table). Thus, *pin7* and *pin1* mutants displayed defects in establishing the apical and basal embryo poles at the sites of auxin response, which were not within, but adjacent to, the expression domains of polarly localized PIN1 and PIN7.

Functional redundancy among PIN proteins

Despite strong defects in early embryos, the majority of *pin7* mutants recovered and produced fertile plants that showed only mild auxin-related defects (not shown). This recovery coincided with the onset of PIN1 and PIN4 polar localization, suggesting functional redundancy among *PIN* genes. Therefore, we constructed double, triple and quadruple combinations of *pin7* with *pin1*, *pin3* and *pin4* mutants to generate loss of function of all embryonically expressed *PIN* genes. *pin4 pin7* showed apical defects that persisted into the seedling stage, such as aberrant cotyledon number (Fig. 4q), which were found in none of the single mutants. Stronger defects were observed in triple mutants; for example, apical defects including fused cotyledons and a very short root in *pin1 pin3 pin4* seedlings (Fig. 4r). *pin1 pin3 pin4 pin7* quadruple mutants showed pronounced defects in proembryo establishment, forming shrunken, filamentous or multi-layered structures at early stages (Fig. 4p). Later on, quadruple mutants failed to recover, in contrast to *pin7*, and produced malformed globular embryos. The terminal phenotype of quadruple mutants was variable (Supplementary Table). Most embryos displayed misplaced or fused cotyledons, deletion of apical structures and pronounced root pole defects. Some embryos completely failed to establish apical–basal polarity and were ball-shaped (Fig. 4p). Depending on the ecotype background, quadruple mutants were either embryo lethal or developed into seedlings with severe apical defects and no or a non-functional root (Fig. 4s, t). The aberrations in quadruple embryos were similar to the defects in embryos after interfering with auxin homeostasis (see Fig. 2h, i) or those in *gn* embryos (Fig. 4p, t, insets). Furthermore, *gn* embryos and seedlings show the same range of phenotypes as *pin* quadruple mutants (Supplementary Table). Thus, analysis of multiple mutants demonstrated functional redundancy among PIN proteins and identified PIN-dependent auxin transport as an essential mechanism for the recovery of the apical–basal axis in *pin7* mutants at later stages of embryogenesis.

Discussion

The analysis of axis formation in genetically tractable animal models, such as *Drosophila* and *Caenorhabditis*, has been greatly facilitated by the accessibility of the freshly laid egg to experimental manipulation. By contrast, flowering-plant embryos develop deep inside maternal tissues, seriously limiting a comparable approach. Although a molecular analysis of *Arabidopsis* genes involved in early patterning suggested a link to the plant signalling molecule auxin, the spatial and temporal requirement for auxin in embryogenesis and its role in axis formation were not shown. We have succeeded

in visualizing auxin and its response in early embryogenesis. The *in vitro* culture of *Arabidopsis* embryos enabled us to combine mutant and marker analysis with experimental interference of auxin homeostasis. This approach, in conjunction with a molecular analysis of auxin transport during early embryogenesis, proved to be instrumental in elucidating the mechanism of axis formation in plants.

Our results show a dynamic distribution of auxin and its response, and suggest routes of auxin transport during early embryogenesis (Fig. 5). Immediately after division of the zygote, auxin accumulates in the smaller apical cell, auxin response is activated and the cell is specified as founder of the proembryo (Fig. 5a). Auxin is actively provided here from the adjacent basal cell by PIN7-dependent transport, as both chemical efflux inhibition and *pin7* mutations cause failure of the establishment of the apical–basal auxin gradient and lead to auxin accumulation in the basal cell. Moreover, PIN7 is polarly localized to the apical plasma membrane of the basal cell, where it is perfectly positioned to provide auxin to the adjacent apical cell. This apical–basal auxin distribution mediates correct specification of the apical cell, because this specification is compromised in *pin7* and even more strongly in quadruple *pin* mutants as demonstrated by aberrations in both cell behaviour and marker expression. Thus, an actively maintained PIN-dependent auxin gradient is required for the specification of the apical cell, which later becomes the founder of the proembryo and all apical structures of the plant.

At the globular stage (Fig. 5b), bioactive auxin production probably starts in the apical embryo region. In support of this, auxin response is activated ectopically in this region following chemical inhibition of auxin transport or in *gn* mutants. At the same stage, PIN1 basal localization is established in the provascular cells, suggesting downward transport towards the region of the future root pole. Simultaneously, the asymmetric localization of PIN7 is reversed within the basal cells, mediating auxin transport out of the embryo. Subsequently, PIN4 expression starts at the basal pole of the embryo, supporting the action of both PIN1 and PIN7 (Fig. 5b). The PIN7-dependent auxin transport in the suspensor operates at a lower rate than that mediated by PIN1 and PIN4. As a result, the auxin gradient reverses, displaying its new maximum in
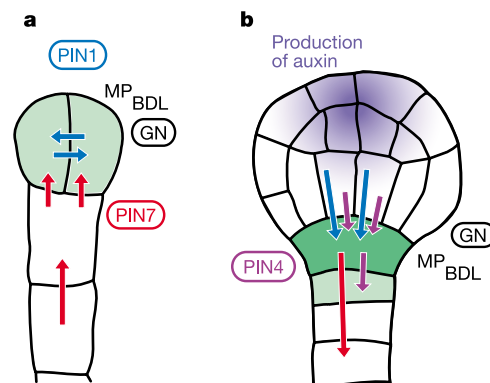
Figure 5 A model for a role of auxin in embryo patterning. Sites of auxin response and accumulation are shown in green. Arrows indicate routes of auxin efflux mediated by PIN1 (blue), PIN4 (purple) or PIN7 (red). Also depicted are proteins involved in embryo patterning and related to auxin transport (GN, encircled) or response (BDL, MP). **a**, Two-cell-stage embryo. Auxin accumulates in the proembryo through PIN7-dependent transport and triggers apical pole specification. **b**, Young globular embryo. Free auxin starts to be produced in the apical part (purple) and auxin transport routes reverse. Auxin accumulates in a PIN1- and PIN4-dependent manner in the hypophysis, triggering root pole specification.

the uppermost suspensor cell, which in response to auxin is specified to become the hypophysis—the founder of the future root meristem.

At this stage, PIN7 function becomes redundant, because *pin7* mutants recovered and were able to re-establish the axis. This recovery may be akin to *de novo* axis formation in other auxin-dependent processes, such as plant regeneration from callus or postembryonic organ initiation[32]. By contrast, *pin* quadruple mutants failed to recover at this stage and displayed strong *gn*-like defects. In the extreme case, these quadruple mutants were ball-shaped, entirely lacking apical–basal polarity, and the same effects were also caused by chemical inhibition of auxin transport. These findings indicate that the re-establishment of the axis at the globular stage is also mediated by a PIN-dependent auxin distribution, and that this mechanism is probably non-redundant. Thus, axis formation in embryogenesis appears to be a prime example of plant developmental plasticity, involving a self-repairing mechanism of auxin gradients.

In summary, our results provide the first coherent conceptual framework of how the apical–basal axis is established in plants. This process starts with the asymmetric cell division of the zygote, which generates auxin-transporting and auxin-responsive daughter cells. It is conceivable that this first step of axis initiation depends on the auxin transport from the maternal tissue into the zygote; however, owing to a lack of experimental data, this question remains open. Nonetheless, the elaboration of this initial axis is clearly auxin-dependent, because immediately an actively maintained auxin activity gradient is formed, which triggers first the specification of the apical pole and, after its reversal, that of the basal embryo pole. Thus, axis formation in plants involves active accumulation of a signalling molecule by efflux from polarized cells and a localized response. Active accumulation of a signalling molecule results in an inverse gradient with a maximum away from the source, in contrast to the known mechanisms of axis formation in other systems, which involve signalling molecules whose concentration steadily decreases from a maximum at the site of production[33,34]. □

Methods

Materials

DR5rev::GFP consists of nine repeats of the auxin-response element (TGTCTC) fused in inverse orientation to the CaMV minimal 35S promoter[35] and the ER-targeted eGFP coding sequence (Clontech). GAL4/*UAS* constructs for *DR5* expression of DTA were generated as described[27]. Mutant lines of *gn*[4], *mp*[4], *bdl*[5], *pin1* (ref. 20) and *pin4-3* (ref. 13) have been described. Full-length coding sequences of *PIN6* and *PIN7* (GenBank accession numbers AF087819 and AF087820), *PIN5* and *PIN8* were isolated from cDNA libraries prepared from seedlings, leaves and whole plants. *PIN7* RNAi plants expressed, from the CaMV 35S promoter, a construct spanning nucleotides 870–1,344 of *PIN7* cDNA sequence in both sense and antisense orientation, joined by the *uidA* coding sequence. *pin7-1*, *-3* mutant lines with sequence-indexed insertions were identified in the Cold Spring Harbor gene-trap library (http://genetrap.cshl.org/) and *pin7-2*, *pin3-4*, *pin3-5* in the Signal Insertion Mutant Library (http://signal.salk.edu/cgi-bin/tdnaexpress/). *pin7-1*, *-2* and *-3* insertions were at positions 1,349, 1,836 and 2,174 from ATG, respectively. *pin3-4* and *-5* insertions were at positions 1,014 and −51 from ATG, respectively. The *PIN7* enhancer-trap line from a library generated in our laboratory had the *Ds-GUS* transposon inserted at position 1,851 behind the *PIN7* stop codon. The *pin1 pin3 pin4 pin7* quadruple mutant was generated from *pin1*, *pin3-5*, *pin4-3* and *pin7-1* lines.

Growth conditions and microscopy

Plants were grown in a 16 h light/8 h dark cycle at 25/20 °C. For *in vitro* embryo culture, excised ovules were placed on ×0.5 MS media containing 2% sucrose, 400 mg l^{-1} glutamine and 0.3% Phytagel. For treatments, this medium was supplemented with 20–50 μM of NAA, 2,4-D or NPA, or 10–20 μM of BFA. Plates were kept in the dark at 22 °C for up to 7 days. At different times, embryos were excised from the ovules for microscopic analysis. For each condition and stage, at least 40 embryos were analysed. Schiff staining was performed as described[36]. For all treatments, markers and mutant phenotype analyses, we performed control experiments in the sister lines and analysed a sufficient number of embryos (see Supplementary Information). Microscopy was done on a Zeiss Axiophot equipped with an Axiocam HR CCD camera using differential interference contrast optics or epifluorescence. For confocal laser scanning microscopy, a Leica TCS SP was used. Images were processed in Adobe Photoshop.

Expression and immunolocalization analyses

For GFP visualization, samples were mounted in 5% glycerol without fixation and inspected. Histochemical GUS activity staining was performed using a modified indigogenic method[27]. *PIN2::GUS*[37], *PIN3::GUS*[22] and *PIN4::GUS*[13] have been described. *PIN1::GUS* and *PIN6::GUS* constructs were generated by fusing a polymerase chain reaction (PCR)-amplified fragment (nucleotides −1,289 to −5; −1,794 to −1) with the *uidA* gene. The *PIN7:GUS* translational fusion was generated by fusing *uidA* gene to the carboxy terminus of the *PIN7* coding sequence. *In situ* hybridization was performed as described[7] with probes corresponding to cDNA regions of *PIN1* (nucleotides 679–1,149), *PIN3* (999–1,449) and *PIN7* (608–1,456). Anti-PIN1 (ref. 38), anti-PIN4 (ref. 13) and anti-IAA[28] (Phytodetek, Agdia) antibodies have been described. Anti-PIN7 antibodies were raised against recombinant proteins corresponding to amino acids 204 to 486 of PIN7, and were affinity-purified as described[38]. Immunolocalization was done as described[8,37]. Anti-PIN4, anti-PIN1 and anti-PIN7 antibodies were diluted 1:500, 1:200 and 1:50, respectively. Secondary fluorescein isothiocyanate (FITC)- or CY3-conjugated goat anti-rabbit antibodies (Dianova) were diluted 1:200 or 1:600, respectively. IAA immunolocalization[39] in embryos was done after prefixation with 3% 1-ethyl-3-(3-dimethylaminopropyl)carbodiimide hydrochloride (EDAC, Sigma) for 1 h. Anti-IAA antibody and secondary alkaline phosphatase-conjugated anti-mouse antibody (Novagen) were diluted 1:500 and 1:1,000, respectively.

1. St Johnston, D. & Nüsslein-Volhard, C. The origin of pattern and polarity in the *Drosophila* embryo. *Cell* **68**, 201–219 (1992).
2. Lyczak, R., Gomes, J. & Bowerman, B. Heads or tails: cell polarity and axis formation in the early *Caenorhabditis elegans* embryo. *Dev. Cell* **3**, 157–166 (2002).
3. Jürgens, G. Apical–basal pattern formation in *Arabidopsis* embryogenesis. *EMBO J.* **20**, 3609–3616 (2001).
4. Mayer, U., Torres Ruiz, R. A., Berleth, T., Miséra, S. & Jürgens, G. Mutations affecting body organization in the *Arabidopsis* embryo. *Nature* **353**, 402–407 (1991).
5. Hamann, T., Mayer, U. & Jürgens, G. The auxin-insensitive *bodenlos* mutation affects primary root formation and apical–basal patterning in the *Arabidopsis* embryo. *Development* **126**, 1387–1395 (1999).
6. Hardtke, C. & Berleth, T. The *Arabidopsis* gene *MONOPTEROS* encodes a transription factor mediating embryo axis formation and vascular development. *EMBO J.* **17**, 1405–1411 (1998).
7. Hamann, T., Benkova, E., Bäurle, I., Kientz, M. & Jürgens, G. The *Arabidopsis BODENLOS* gene encodes an auxin response protein inhibiting MONOPTEROS-mediated embryo patterning. *Genes Dev.* **16**, 1610–1615 (2002).
8. Steinmann, T. et al. Coordinated polar localization of auxin efflux carrier PIN1 by GNOM ARF-GEF. *Science* **286**, 316–318 (1999).
9. Geldner, N. *et al.* The *Arabidopsis* GNOM ARF-GEF mediates endosomal recycling, auxin transport, and auxin-dependent plant growth. *Cell* **112**, 219–230 (2003).
10. Liu, C., Xu, Z. & Chua, N. Auxin polar transport is essential for the establishment of bilateral symmetry during early plant embryogenesis. *Plant Cell* **5**, 621–630 (1993).
11. Hadfi, K., Speth, V. & Neuhaus, G. Auxin-induced developmental patterns in *Brassica juncea* embryos. *Development* **125**, 879–887 (1998).
12. Sabatini, S. *et al.* An auxin-dependent distal organizer of pattern and polarity in the *Arabidopsis* root. *Cell* **99**, 463–472 (1999).
13. Friml, J. *et al.* AtPIN4 mediates sink-driven auxin gradients and root patterning in *Arabidopsis*. *Cell* **108**, 661–673 (2000).
14. Fischer-Iglesias, C., Sundberg, B., Neuhaus, G. & Jones, A. Auxin distribution and transport during embryonic pattern formation in wheat. *Plant J.* **26**, 115–129 (2001).
15. Ribnicky, D., Cohen, J., Hu, W. & Cooke, T. An auxin surge following fertilization in carrots: a mechanism for regulating plant totipotency. *Planta* **214**, 505–509 (2002).
16. Friml, J. Auxin transport—shaping the plant. *Curr. Opin. Plant Biol.* **6**, 7–12 (2003).
17. Rubery, P. & Sheldrake, A. Carrier-mediated auxin transport. *Planta* **118**, 101–121 (1974).
18. Raven, J. Transport of indolacetic acid in plant cells in relation to pH and electrical potential gradients, and its significance for polar IAA transport. *New Phytol.* **74**, 163–172 (1975).
19. Friml, J. & Palme, K. Polar auxin transport—old questions and new concepts? *Plant Mol. Biol.* **49**, 273–284 (2002).
20. Okada, K., Ueda, J., Komaki, M., Bell, C. & Shimura, Y. Requirement of the auxin polar transport system in early stages of *Arabidopsis* floral bud formation. *Plant Cell* **3**, 677–684 (1991).
21. Rashotte, A., Brady, S., Reed, R., Ante, S. & Muday, G. Basipetal auxin transport is required for gravitropism in roots of *Arabidopsis*. *Plant Physiol.* **122**, 481–490 (2000).
22. Friml, J., Wisniewska, J., Benková, E., Mendgen, K. & Palme, K. Lateral relocation of auxin efflux regulator AtPIN3 mediates tropism in *Arabidopsis*. *Nature* **415**, 806–809 (2002).
23. Ottenschläger, I. *et al.* Gravity-regulated differential auxin transport from columella to lateral root cap cells. *Proc. Natl Acad. Sci. USA* **100**, 2987–2991 (2003).
24. Yamaizumi, M., Mekada, E., Uchida, T. & Okada, Y. One molecule of Diptheria Toxin fragment A introduced into a cell can kill the cell. *Cell* **15**, 245–250 (1978).
25. Haseloff, J. GFP variants for multispectral imaging of living cells. *Methods Cell Biol.* **58**, 139–151 (1999).
26. Weijers, D., Geldner, N., Offringa, R. & Jürgens, G. Early paternal gene activity in *Arabidopsis*. *Nature* **414**, 709–710 (2001).
27. Weijers, D. *Hormonal Regulation of Pattern Formation in the* Arabidopsis *Embryo*. Thesis, Univ. Leiden (2002).
28. Caruso, J., Pence, V. & Leverone, L. in *Plant Hormones: Physiology, Biochemistry and Molecular Biology* (ed. Davies, P.) 43–447 (Kluwer Academic, The Netherlands, 1995).
29. Delbarre, A., Muller, P., Imhoff, V. & Guern, J. Comparison of mechanisms controlling uptake and accumulation of 2,4-dichlorophenoxy acetic acid, naphthalene-1-acetic acid, and indole-3-acetic acid in suspension-cultured tobacco cells. *Planta* **198**, 532–541 (1996).
30. Sundaresan, V. *et al.* Patterns of gene action in plant development revealed by enhancer trap and gene trap transposable elements. *Genes Dev.* **14**, 1797–1810 (1995).
31. Mayer, U., Büttner, G. & Jürgens, G. Apical–basal pattern formation in the *Arabidopsis* embryo: Studies on the role of the *gnom* gene. *Development* **117**, 149–162 (1993).
32. Steeves, T. & Sussex, I. *Patterns in Plant Development* (Cambridge Univ. Press, Cambridge, 1989).

33. Teleman, A., Strigini, M. & Cohen, S. Shaping morphogen gradients. *Cell* **105,** 559–562 (2001).
34. Tabata, T. Genetics of morphogen gradients. *Nature Rev. Genet.* **2,** 620–630 (2001).
35. Ulmasov, T., Murfett, J., Hagen, G. & Guilfoyle, T. Aux/IAA proteins repress expression of reporter genes containing natural and highly active synthetic auxin response elements. *Plant Cell* **9,** 1963–1971 (1997).
36. Braselton, J., Wilkinson, M. & Clulow, S. Feulgen staining of intact plant tissues for confocal microscopy. *Biotechnol. Histochem.* **71,** 84–87 (1996).
37. Friml, J., Benkova, E., Mayer, U., Palme, K. & Muster, G. Automated whole mount localisation techniques for plant seedlings. *Plant J.* **34,** 115–124 (2003).
38. Gälweiler, L. *et al.* Regulation of polar auxin transport by AtPIN1 in *Arabidopsis* vascular tissue. *Science* **282,** 2226–2230 (1998).
39. Moctezuma, E. Changes in auxin patterns in developing gynophores of the peanut plant (*Arachis hypogaea* L.). *Ann. Bot.* **83,** 235–242 (1999).

Supplementary Information accompanies the paper on **www.nature.com/nature**.

Competing interests statement The authors declare that they have no competing financial interests.

Correspondence and requests for materials should be addressed to J.F. (jiri.friml@zmbp.uni-tuebingen.de).